Contents lists available at ScienceDirect

Biological Conservation

journal homepage: www.elsevier.com/locate/biocon

Tropical rays are intrinsically more sensitive to overfishing than the temperate skates

Ellen Barrowclift [a,*], Sarah M. Gravel [b], Sebastián A. Pardo [c], Jennifer S. Bigman [d], Per Berggren [a,*], Nicholas K. Dulvy [b]

[a] *School of Natural and Environmental Sciences, Newcastle University, Newcastle-upon-Tyne, United Kingdom*
[b] *Earth to Ocean Research Group, Department of Biological Sciences, Simon Fraser University, Burnaby, British Columbia V5A 1S6, Canada*
[c] *Ecology Action Centre, Halifax, Nova Scotia, BSK 4L3, Canada*
[d] *Alaska Fisheries Science Center, NOAA, Seattle, United States*

ABSTRACT

Overfishing, habitat loss, and climate change are driving population declines in many species. Understanding a species' capacity to recover from these and other threats is necessary for prioritising management. The maximum intrinsic rate of population increase (r_{max}) can be used to compare which species or groups are particularly sensitive to ongoing threats. To investigate global patterns of intrinsic sensitivity of rays and skates (superorder Batoidea), we calculated r_{max} of 85 species using a modified Euler-Lotka model that accounts for survival to maturity. We examined how r_{max} varies with body mass, temperature, and depth using an information-theoretic approach through model selection, accounting for phylogenetic non-independence. Although we observed an overall positive relationship between r_{max} and temperature, we found that warm, shallow-water rays were more intrinsically sensitive to exploitation (lower r_{max}) than cold, deep-water skates (higher r_{max}). We hypothesise that this pattern is likely driven by their different reproductive strategies as live-bearing rays have fewer offspring compared to egg-laying skates, and caution that future research should focus on understanding differences in the mortality schedule of juveniles and sub-adults to understand if survival to maturity is comparable. Our findings highlight the high vulnerability of warm, shallow-water ray species to overexploitation and other threats due to their intrinsically low maximum population growth rates. These differences in r_{max} have conservation implications for our understanding of the geographic patterns in extinction risk, suggesting that tropical rays are more intrinsically sensitive.

1. Introduction

Understanding population growth rate is central to understanding species' responses to overfishing, habitat loss and degradation, and climate change (Webb et al., 2011; Yan et al., 2021). Species' vulnerability is a combination of intrinsic sensitivity and extrinsic exposure to fishing and other threats (Dulvy and Kindsvater, 2017; Juan-Jordá et al., 2015). Intrinsic sensitivity can be indexed by the maximum intrinsic rate of population increase (r_{max}), which in its simplest form, can be calculated from age at maturity, maximum age, and annual reproductive output. r_{max} represents the theoretical maximum intrinsic population growth rate at low population sizes, i.e., in the absence of density-dependent processes (Cortés et al., 2015; Myers et al., 1999, 1997; Pardo et al., 2018) and is equal to the fishing mortality that will cause a

species or population to become extinct ($F_{extinct}$) (Dulvy et al., 2004; Gedamke et al., 2007). Understanding how r_{max} varies among species can therefore inform our understanding of sensitivity to exploitation, recovery potential, and can also be used as a Bayesian prior to help estimate catch limits in fisheries stock assessments (Martell and Froese, 2013; Patrick et al., 2010).

Chondrichthyans (shark, rays, and chimaeras; hereafter, referred to as 'sharks and rays ') are a highly threatened taxon, with over one-third of species threatened with extinction (The International Union for the Conservation of Nature's (IUCN) Red List of Threatened Species categories of Vulnerable, Endangered, or Critically Endangered) due to overfishing (Dulvy et al., 2021). Sharks and rays are important sources of income and protein in the fisheries that are causing their decline, particularly small-scale fisheries in developing countries that comprise

over 95 % of the world's fishers (Béné, 2006; Pauly, 2006; Temple et al., 2019). Ensuring sustainability is crucial for both food security and healthy marine ecosystems (Barrowclift et al., 2017; Simpfendorfer and Dulvy, 2017). Sharks and rays typically have slow life histories including low somatic growth rates, late maturity, and low fecundity that result in relatively low r_{max} estimates (Cortés, 2000; García et al., 2008). Combined with limited density-dependent compensation in juvenile survival due to their narrow range of annual reproductive output, sharks and rays are extremely sensitive to elevated mortality from fisheries (Cortés, 2002; Dulvy and Forrest, 2010; Quetglas et al., 2016). There is, however, wide variation in life histories among sharks and rays, and even within rays there may be a range of r_{max} estimates that indicate their differing resilience to exploitation (Hutchings et al., 2012; Quetglas et al., 2016; Ward-Paige, 2017). Rays of the superorder Batoidea are comprised of both live-bearing rays (Torpedo rays, Torpediniformes; Rhino rays, Rhinopristiformes; and stingrays, Myliobatiformes) and egg-laying skates (Rajiformes). Hereafter, we refer to these two lineages as "rays' and "skates', respectively. Live-bearing rays have much lower fecundities than egg-laying skates (Goodwin et al., 2002), probably limited by maternal body size (Musick and Ellis, 2005; Wourms, 1977; Wourms and Lombardi, 1992), whilst egg-laying skates face increased mortality from predation on eggs (Lucifora and García, 2004; Powter and Gladstone, 2008). Low fecundity likely limits r_{max} estimates (Pardo et al., 2018) and represents differences in reproductive allocation that influences population growth rates and generation lengths (Cortés, 2002; Juan-Jordá et al., 2013).

Maximum body size is a widely available predictor of extinction risk, with larger-bodied species typically at greater risk of decline and extinction due to slow life histories and low r_{max} estimates (Hutchings et al., 2012; Jennings et al., 1998; Reynolds et al., 2005). However, where sufficient data allow, broader time-related life history traits including age at maturity, somatic growth rates, longevity and mortality rates have been found to better explain life history variation and better correlate with extinction risk across different taxonomic groups (Anderson et al., 2011; Chichorro et al., 2019; Juan-Jordá et al., 2015). Theoretically and empirically, r_{max} has been shown to scale with body mass and temperature across taxa. This is likely due to r_{max} being closely tied to metabolic rate and trade-offs in energy allocated to survival, growth, and reproduction (Savage et al., 2004; White et al., 2022; Wong et al., 2021), such that r_{max} has been found to decrease with increasing body size in sharks and rays (Dulvy et al., 2014; Hutchings et al., 2012; Pardo and Dulvy, 2022). The expectation is that organisms with a higher metabolic rate in warmer waters (tropical, low latitudes) will tend towards 'faster' life histories, growing quickly to a smaller maximum body size (Healy et al., 2019; Reynolds, 2003), and consequently, have a higher r_{max} than those with slower metabolic rates and 'slower' life histories in cooler waters (temperate and polar, high latitudes) (Brown et al., 2004; Clarke and Johnston, 1999; Juan-Jordá et al., 2013). These temperature-related, latitudinal patterns may also be evident along depth gradients as temperatures generally decrease with increasing depth. Indeed, deep-water shark and ray species tend to have slower life histories and lower r_{max} estimates compared to continental shelf and pelagic species (García et al., 2008; Pardo and Dulvy, 2022; Simpfendorfer and Kyne, 2009).

Contrary to metabolic scaling expectations, there are some warm, shallow-water tropical rays, notably the filter-feeding devil rays (*Mobula* spp.), that have extremely low r_{max} (Dulvy et al., 2014; Pardo et al., 2016a). Pardo and Dulvy (2022) found that as body size increases, decreases in r_{max} were much steeper for warmer-water species, suggesting that a greater intrinsic sensitivity may also be playing a role in the higher extinction risk of tropical rays (Dulvy et al., 2021). Thus far, r_{max} estimates have been made for only a few ray and skate species (Barbini et al., 2021; Barnett et al., 2013; D'Alberto et al., 2019; Dulvy et al., 2014; Lucifora et al., 2022; Pardo et al., 2016b; Temple et al., 2020).

Here, we calculate r_{max} for 85 ray and skate species using available life history data. We then use an information-theoretic approach,

accounting for phylogenetic non-independence of species, to investigate how body mass, temperature, and depth may explain variation in r_{max} estimates for rays and skates.

2. Methods

First, we summarise data sources, including our literature search for life history data and methods used to estimate r_{max}. Second, we outline methods for obtaining body mass, depth, and temperature data. Third, we describe our analytical approach, including the metabolic scaling expectations and the statistical models associated with each hypothesis.

2.1. Collation of life history trait data and estimation of r_{max}

A database of published life history data for rays and skates was collated up to the date of submission of this manuscript. The database was developed from the generation lengths used in the recent IUCN Red List reassessments (Dulvy et al., 2021). To collate life history traits, searches were conducted in Web of Science and Google Scholar using the following search terms: age/growth/maturity/fecundity/litter size/life history/maximum intrinsic rate of population increase/productivity/ reproductive biology AND ray* (wild character to return ray and rays) 'AND chondrichthy*' (wild character to return Chondrichthyes and chondrichthyan). The term 'ray*' has additional non-relevant usages so 'AND chondrichthy*' was added to the search term. The IUCN Red List (www.iucnredlist.org/) was also used to check species-specific life history parameters using information available in the 'Habitat and Ecology' tab, with references checked from the 'Bibliography' tab. Data were also taken from the life history database Sharkipedia (https://www.sharkip edia.org/) (Mull et al., 2022). Taxonomy was checked against Eschmeyer's Catalog of Fishes (https://researcharchive.calacademy.or g/research/ichthyology/catalog/fishcatmain.asp). We assigned life history data sourced from the literature to the most updated taxonomic nomenclature based on geographic distribution.

To estimate r_{max}, we used a modified Euler-Lotka model that accounts for survival to maturity with the following equation (Cortés, 2016; Pardo et al., 2018, 2016b):

$$l_{\alpha_{mat}}b = e^{r_{max}\alpha_{mat}} - e^{-M}\left(e^{r_{max}}\right)^{\alpha_{mat}-1}, \tag{1}$$

where $l_{\alpha_{mat}}$ is the proportion of individuals surviving to maturity, which is calculated with $l_{\alpha_{mat}} = (e^{-M})^{\alpha_{mat}}$, b is annual fecundity, M is the species-specific instantaneous natural mortality rate and α_{mat} is the age at maturity. We used a simple estimate of natural mortality (M) that is equivalent to the reciprocal of average lifespan, estimated with $M = 1/\omega$ (Dulvy et al., 2004; Pardo et al., 2016a, 2016b), where ω is an estimate of average lifespan in years. Average lifespan was assumed to be the midpoint between age at maturity (α_{mat}) and maximum age (α_{max}) (Pardo et al., 2016b), estimated with:

$$\omega = \frac{(\alpha_{max} + \alpha_{mat})}{2} \tag{2}$$

For this, we searched for age at maturity (female age at 50 % maturity, years; α_{mat}), maximum age (recorded for females where known, years; α_{max}), and annual reproductive output (number of female offspring assuming 1:1 sex ratio; b). Because these life history traits can vary within species and thus result in uncertainty in r_{max}, we calculated 10,000 random deviates from a uniform distribution between minimum and maximum values of each life history parameter. We then estimated r_{max} with each of the life history values and took the median to generate a species-specific r_{max} value. Uncertainty in this r_{max} value was estimated as the 2.5 % and 97.5 % quantiles. If only point estimates were available, such as for α_{max}, then 10 % was subtracted and added to get a minimum and maximum value, respectively. Where regional differences in life history trait data were described in the IUCN Red List assessments (n = 7 species), r_{max} was calculated for each location and then a mean

r_{max} for that species was used in further analyses.

2.2. Body mass, depth, and temperature-at-depth data

The maximum reported body mass (in grams) for each species was extracted from FishBase (Froese and Pauly, 2022) using the *rfishbase* package (Boettiger et al., 2012). Where maximum body mass data were unavailable, length-weight conversions available on FishBase were used to convert maximum length (cm) to weight (g). Data sourced from FishBase were manually checked from the original references and updated where necessary. Length-weight regression coefficient estimates were selected for females where possible and for the most appropriate length-measurement type (disc width or total length) depending on the species' body shape. If a length-weight conversion was unavailable for a species, then a length-weight conversion for a closely related species with a similar maximum size and body shape was used. Finally, there were two species where length-weight conversions were calculated from the Bayesian models available on FishBase (Froese et al., 2014).

Median depth estimates for each species were taken as the midpoint of the minimum and maximum depth ranges reported in the IUCN Red List Assessment of Threatened Species as reported in Dulvy et al. (2021). Temperature-at-depth was then determined using species geographic range shape files available as part of a global reassessment of shark and ray species (see Dulvy et al. (2021) page e6 for details of distribution mapping and Data S3 for data sources available on the IUCN Red List of Threatened Species). Species distribution was overlaid with the International Pacific Research Center's interpolated dataset of gridded mean annual ocean temperatures across 27 depth levels (0–2000 m below sea level), which is based on measurements from the Argo Project (data available at http://apdrc.soest.hawaii.edu/projects/Argo/data /statistics/On_standard_levels/Ensemble_mean/1x1/m00/index.html). The depth level that was closest to the species' median depth was selected from the grid and the temperature grid points were extracted across the species' distribution. Median temperature for each species was calculated from the distribution of temperature values.

2.3. How does r_{max} vary with body mass, temperature, and depth?

Across taxa, r_{max} has been shown to be related to body mass and temperature (Savage et al., 2004). These metabolic scaling expectations can be estimated with a linear model in natural logarithm (ln):

$$ln(r_{max}) = \beta_0 + \beta_1 * ln(M) + \beta_2 * \frac{1}{k_B T}, \qquad (3)$$

where r_{max} is the maximum intrinsic rate of population increase (year^{-1}), β_0 is the intercept, β_1 is the mass-scaling coefficient, β_2 is the

Table 1
The 24 models examined with associated hypotheses for how maximum intrinsic rate of population increase (r_{max}) varies with body mass, temperature, depth and a composite temperature and depth index. The expected model from metabolic scaling theory is highlighted in grey. Note, Order was categorical for rays (Orders Myliobatiformes, Rhinopristiformes, and Torpediniformes) and skates (Order Rajiformes).

Model	Hypothesis
$ln(r_{max}) \sim 1$	r_{max} only
$ln(r_{max}) \sim ln(M)$	r_{max} varies with body mass only
$ln(r_{max}) \sim depth$	r_{max} varies with depth only
$ln(r_{max}) \sim 1/k_B T$	r_{max} varies with temperature only
$ln(r_{max}) \sim$ temperature-depth index	r_{max} varies with temperature-depth index only
$ln(r_{max}) \sim ln(M) + depth$	r_{max} varies with body mass and depth
$ln(r_{max}) \sim ln(M) + 1/k_B T$	r_{max} varies with body mass and temperature
$ln(r_{max}) \sim ln(M) + temperature-depth\ index$	r_{max} varies with body mass and temperature-depth index
$ln(r_{max}) \sim ln(M) * depth$	r_{max} varies with body mass and depth, and the effect of mass scaling coefficient varies with depth
$ln(r_{max}) \sim ln(M) * 1/k_B T$	r_{max} varies with body mass and temperature, and the effect of mass scaling coefficient varies with temperature
$ln(r_{max}) \sim ln(M) * temperature-depth\ index$	r_{max} varies with body mass and temperature-depth index, and the effect of mass scaling coefficient varies with the temperature-depth index
$ln(r_{max}) \sim 1 + Order$	r_{max} varies with Order
$ln(r_{max}) \sim ln(M) + Order$	r_{max} varies with body mass and Order
$ln(r_{max}) \sim depth + Order$	r_{max} varies with depth and Order
$ln(r_{max}) \sim 1/k_B T + Order$	r_{max} varies with temperature and Order
$ln(r_{max}) \sim temperature-depth\ index + Order$	r_{max} varies with temperature-depth index and Order
$ln(r_{max}) \sim ln(M) + depth + Order$	r_{max} varies with body mass, depth, and Order
$ln(r_{max}) \sim ln(M) + 1/k_B T + Order$	r_{max} varies with body mass, temperature, and Order
$ln(r_{max}) \sim ln(M) + temperature-depth\ index + Order$	r_{max} varies with body mass, temperature-depth index, and Order
$ln(r_{max}) \sim ln(M) * depth + Order$	r_{max} varies with body mass, depth, and Order, and the effect of mass scaling coefficient varies with depth
$ln(r_{max}) \sim ln(M) * 1/k_B T + Order$	r_{max} varies with body mass, temperature, and Order, and the effect of mass scaling coefficient varies with temperature
$ln(r_{max}) \sim ln(M) * temperature-depth\ index + Order$	r_{max} varies with body mass, temperature-depth index, and Order, and the effect of mass scaling coefficient varies with the temperature-depth index
$ln(r_{max}) \sim ln(M) + 1/k_B T + depth$	r_{max} varies with body mass, temperature, and depth
$ln(r_{max}) \sim ln(M) + 1/k_B T * depth$	r_{max} varies with body mass and the effect of temperature varies with depth

activation energy E, T is the temperature (in Kelvin) and k_B is the Boltzmann constant (8.617×10^{-5} eV).

Here, 24 models representing alternative hypotheses of how r_{max} may vary with body mass, temperature, and depth were compared using an information-theoretic approach (Burnham and Anderson, 2002) (Table 1). The above equation is the expectation from metabolic scaling theory and is one of the 24 hypotheses compared. r_{max} and adult body mass data were ln-transformed. Temperature and depth data were standardised (scaled and centred) prior to analyses.

Twenty, random phylogenetic trees from the possible distribution of trees from Stein et al. (2018), and available at Vertlife.org, were used in analyses to include a random effect of phylogeny in all models. Note, the phylogeny was updated to reflect current taxonomic nomenclature, for example *Dasyatis americana* and *D. dipterura* in the phylogeny from Stein et al. (2018) were updated to *Hypanus americanus* and *H. diptererus,* respectively. There were two instances where the phylogenetic position of a species (*Aetobatus narutobiei* and *Maculabatis ambigua*) were not known, so the position (i.e., branch length or divergence time) of a closely related species (*A. flagellum* and *Maculabatis gerrardi*, respectively) was used instead. Taxonomic placement was also included as a categorical fixed term in the model to investigate how r_{max} scales with body mass, temperature, and depth in skates (Order Rajiformes) and rays (Orders Myliobatiformes, Rhinopristiformes, and Torpediniformes) given their different life history strategies (particularly high and low annual reproductive output, respectively) and distributions (encompassing different environmental temperatures and depths).

Phylogenetic generalised linear models were fitted to account for non-independence for closely related species using the *pgls* function in the caper package (Orme et al., 2018). In a *pgls* framework, the phylogeny is converted to a covariance matrix, which is included as a random effect and thus accounts for autocorrelation of the residuals due to species sharing various parts of evolutionary trajectories. The strength of the phylogenetic signal (i.e., how strong the residuals were correlated with the covariance matrix) is indicated by Pagel's λ, with a value of 1 meaning the residuals are perfectly correlated with the covariance matrix and a value of 0 meaning no correlation (Revell, 2010).

We assessed how sensitive our results were to the small variation in the random phylogenies used by re-fitting the models with a subset of 20 (randomly chosen) phylogenies available from Stein et al. (2018). The top model was always the same (Table S1 in the Supplementary Materials) and we therefore only report results from using a single tree. We also assessed how sensitive our results were to the larger-bodied rays present in the dataset (body mass ≥ 290 kg, n = 8) by re-fitting models without these eight data points. The top model was the same (Table S2 in the Supplementary Materials) and we therefore only report results using the full dataset.

Depth and temperature were positively correlated (Pearson's $r = 0.75$), with a value higher than a threshold of 0.70 in which collinearity severely distorts model estimation (Dormann et al., 2013). We therefore used Principal Components Analysis (PCA) to collapse the temperature and depth variables into one Principal Component (PC), a composite temperature and depth index (PC1 axis; hereafter, temperature-depth index), that explained 87 % of the variance. The temperature-depth index was included in place of temperature and depth in some models to examine whether a combined metric better explained r_{max} compared to these environmental variables alone (Table 1). We also estimated variance-inflation factors (VIF) to assess collinearity for all coefficients in the models using the *car* package (Fox and Weisberg, 2019). No VIF value was greater than two, except as expected when interactions were included, indicating that our models were robust to collinearity despite the strong correlation between temperature and depth. Models were compared using the corrected Akaike Information Criterion (AICc). If including a parameter improved the model's AICc by less than two units (ΔAICc $\leq$ 2), it was considered relatively uninformative (Arnold, 2010; Burnham and Anderson, 2002). All analyses were run in R version 4.1.2

(R Core Team, 2021) in RStudio (RStudio Team, 2021).

3. Results

Maximum population growth rate, r_{max}, was estimated using collated life history data (α_{max}, α_{mat}, and b) for 85 ray and skate species and r_{max} estimates varied between 0.0213 yr^{-1} (in *Mobula alfredi*) and 1.28 yr^{-1} (in *Raja miraletus*) (Fig. 1). It was evident that there were two groupings of data: warm, shallow-water rays (n = 53) with relatively low annual reproductive output and cold, deep-water skates (n = 32) with higher annual reproductive output (Figs. 1 and 2). Generally, compared to rays, the skates had a later age at maturity (α_{mat}: skates median = 9.20 ± 1.09 SE; rays = 6.0 ± 0.42 SE) and higher annual reproductive output (b: skates median = 29.10 ± 2.17 SE; rays = 3.0 ± 0.28 SE) but there was little difference in longevity (α_{max}: skates median = 15.50 ± 2.02 SE; rays = 16.0 ± 1.28 SE). Consequently, skates had a higher median r_{max} (0.37 yr^{-1} ± 0.05 SE) compared to rays (0.25 yr^{-1} ± 0.03 SE).

Six of the 24 models examined had ΔAICc < 2, providing substantial support for describing variation in r_{max} across species (Burnham and Anderson, 2002) (Table 2). The top model with the greatest support (ΔAICc = 0) was for r_{max} varying with body mass and the temperature-depth index (adjusted R^2 = 0.14). Including taxonomic Order in the relationship between r_{max} and body mass and the temperature-depth index, received approximately 55 % of the support of the top-ranked model and resulted in no increase in adjusted R^2 (adjusted R^2 = 0.14). The 95 % confidence intervals for the coefficient estimate for Order in this model also overlapped zero suggesting that the effect size was not significant (Fig. 3). Including an interaction between body mass and the temperature-depth index received 38 % of the support of the top-ranked model and explained less variation (adjusted R^2 = 0.13). Model results suggest that the temperature-depth index, temperature, or depth can be used interchangeably. Models for r_{max} varying with body mass and temperature and body mass and depth received approximately 50 % of the support of the top-ranked model and accounted for less variation (adjusted R^2 = 0.12). Finally, a model for r_{max} varying with body mass, temperature, and depth, with an interaction term between temperature and depth, received less than half of the support of the top-ranked model (approximately 43 %) and accounted for the same variation (adjusted R^2 = 0.14). Eight other models had moderate support (< 2 ΔAICc ≥ 4), with marginal support for six other models (≤ 5 ΔAICc ≥ 7) (Table 2).

The scaling of body mass in all models was shallower (−0.12 to −0.10) than expected from metabolic scaling theory (−0.33 to −0.25; Table 3; Fig. 3). Temperature had a positive effect on r_{max} as the coefficient of inverse temperature $1/k_BT$ (activation energy E) was consistently negative, suggesting r_{max} is higher in species found in warmer waters (Table 3). The effect of depth was negative across all models suggesting r_{max} is lower in species found at greater depths (Table 3). An overall positive relationship between r_{max} and temperature was evident in both rays and skates (Fig. 4a) and was mirrored by a negative relationship between r_{max} and depth (Fig. 4b), as would be expected from metabolic scaling theory. Although a shallower relationship, there was a negative relationship between r_{max} and body mass when controlling for a constant temperature (Fig. 5a), depth (Fig. 5b), and temperature-depth index (Fig. 6). Whilst r_{max} was found to be lower at greater depths (Fig. 5b) in line with metabolic scaling theory, r_{max} was also found to be lower at warmer temperatures (Fig. 5a), contrary to metabolic scaling expectations. Further, when controlling for a constant temperature-depth index, warm, shallow-water rays showed lower r_{max} compared to cold, deep-water skates (Fig. 6). There was a strong phylogenetic signal from the residuals of r_{max} in all models examined, with Pagel's λ ≥ 0.87 (Table 3).

4. Discussion

We find empirical evidence for a positive relationship between the maximum intrinsic rate of population increase (r_{max}) and temperature.
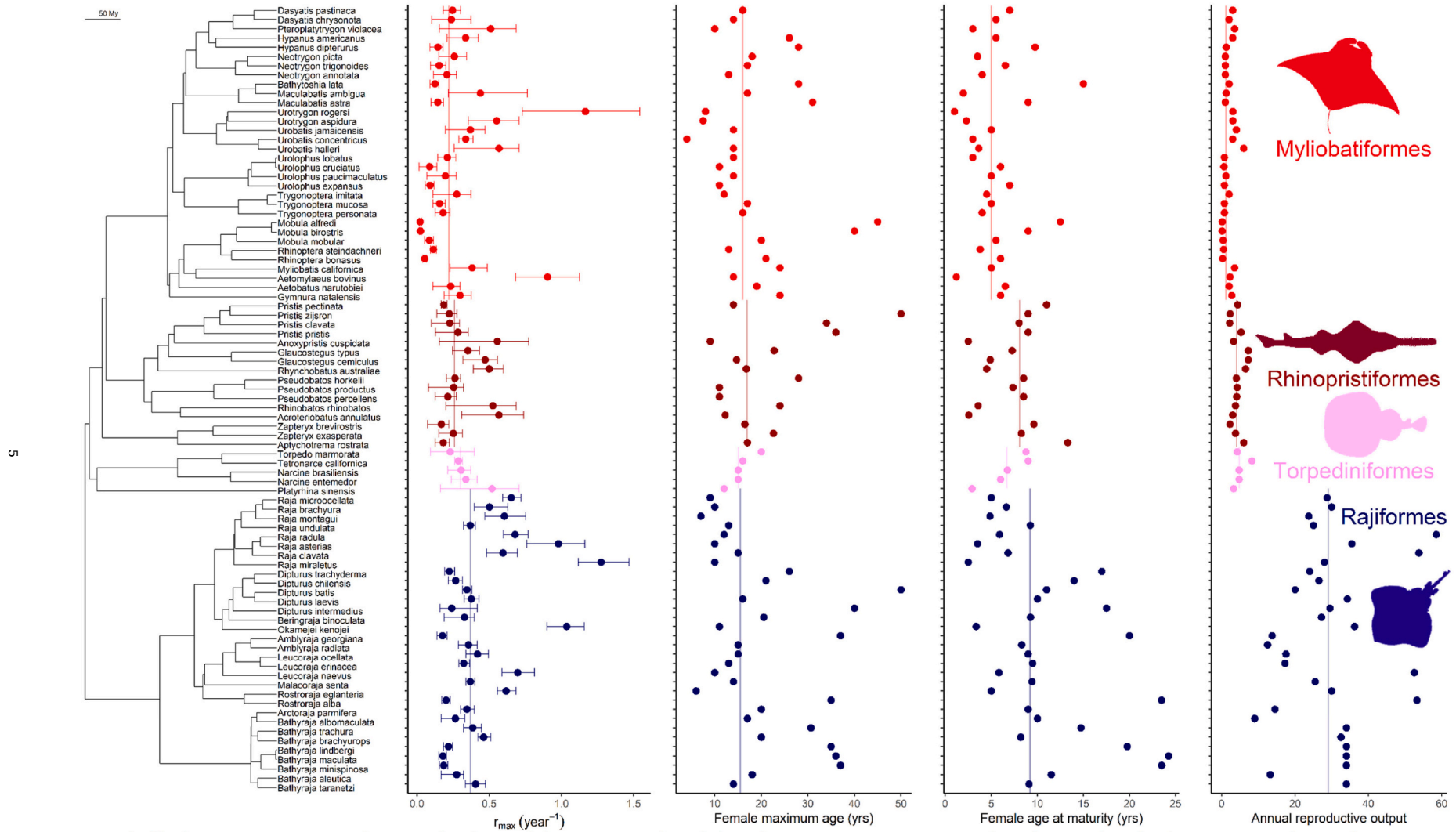
Fig. 1. Phylogeny, maximum intrinsic rate of population increase (r_{max}), female maximum age in years, female age at maturity in years and annual reproductive output (number of female offspring) for 85 ray and skate species. Solid lines show median values for Myliobatiformes (n = 32), Rhinopristiformes (n = 16), Torpediniformes (n = 5) and Rajiformes (n = 32). Uncertainty in r_{max} estimate shown with 2.5 % and 97.5 % quantiles. A single phylogenetic tree from the possible distribution of trees from Stein et al. (2018) is displayed.

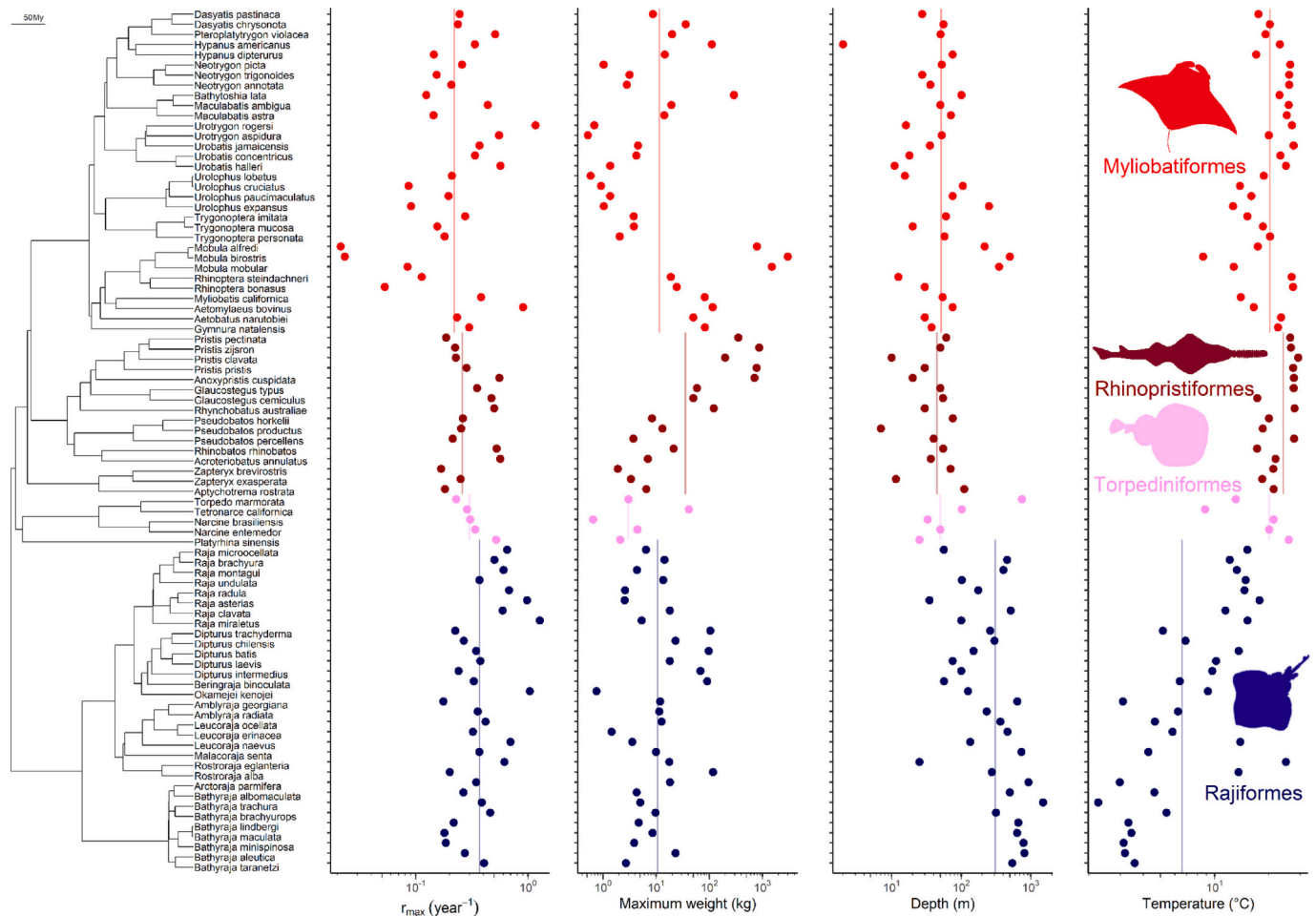**Fig. 2.** Phylogeny, maximum intrinsic rate of population increase (r_{max}), maximum weight (kg), median depth (m) and median temperature (°C) in log10 space for 85 ray and skate species. Solid lines show median values for Myliobatiformes (n = 32), Rhinopristiformes (n = 16), Torpediniformes (n = 5) and Rajiformes (n = 32). A single phylogenetic tree from the possible distribution of trees from Stein et al. (2018) is displayed.

However, paradoxically, the live-bearing, tropical rays have a much lower r_{max} than egg-laying, temperate skates. Metabolic theory and empirical patterns suggest that, after controlling for body size, r_{max} should increase with temperature both among populations and across species (Bernhardt et al., 2018; Luhring and Delong, 2017; Savage et al., 2004). This positive relationship between temperature and r_{max} is consistent with the biogeographic pattern that deep-water species, including sharks, generally have lower r_{max} and are more prone to being overfished than their shallow-water relatives. We found good support for models that included temperature, depth, or a temperature-depth index in the relationship between r_{max} and body mass, such that depth may also be used as a proxy where temperature data may not be available. Below we hypothesise that this paradoxical pattern arises because the cooler, deeper waters are dominated by skates, which are relatively fecund egg-layers, whereas the warmer, shallower waters are dominated by rays, which give birth to few, larger offspring. Next, we discuss (1) the temperature-related biogeography of r_{max}; (2) intrinsic sensitivity to overexploitation and extinction risk; (3) life history correlates of population responses; (4) whether reproductive strategies can explain the r_{max} paradox (that warm, shallow-water tropical rays have lower r_{max} than cold, deep-water skates); (5) fisheries implications, and (6) future research directions.

There are a number of temperature-related, biogeographical patterns in r_{max}. Generally, biological processes are temperature-dependent, for example, metabolic rate increases exponentially with temperature above 15 °C for ectotherms (Clarke, 2017; Clarke and Johnston, 1999;

Dillon et al., 2010). Individual metabolic rate is fundamental to physiological performance and has effects at the population, community, and ecosystem levels (Brown et al., 2004; Pörtner, 2001). Consequently, experimental treatments of algal cultures exhibit increased population growth rates and lower carrying capacity at higher temperatures (Bernhardt et al., 2018; Luhring and Delong, 2017) and comparative analyses reveal that species found at warmer temperatures tend to have higher r_{max} compared to those found at cooler temperatures (Angilletta et al., 2010; Savage et al., 2004). It is therefore not surprising that r_{max} was found to increase with increasing environmental temperature for rays and skates in this study nor that r_{max} decreased with increasing depth. This is in line with theoretical and empirical temperature-related, latitudinal patterns that organisms with higher metabolic rates and 'fast' life histories in warmer waters (tropical, low latitudes) will have higher r_{max}, than those with slower metabolic rates and 'slow' life histories in cooler waters (temperate and polar, high latitudes) (Brown et al., 2004; Clarke and Johnston, 1999; Juan-Jordá et al., 2013). It follows that species with lower r_{max} at cooler, higher latitudes have been found to face greater population declines and therefore higher extinction risk than those with faster life histories at warmer, lower latitudes (Jennings et al., 1999; Juan-Jordá et al., 2015). Similarly, these temperature-related, latitudinal patterns may be evident over a depth gradient. This has been found in sharks, where cooler, deep-water species have a lower r_{max} (Pardo and Dulvy, 2022) and face higher extinction risk and lower population recovery rates (García et al., 2008; Simpfendorfer and Kyne, 2009).

Table 2

Comparison of r_{max} models using corrected Akaike Information Criteria (AICc), number of parameters (n), negative log-likelihood (−LL), adjusted R², and Akaike weights. Models are ordered by ascending AICc, with the top model first and models with ΔAICc < 2 highlighted in grey.

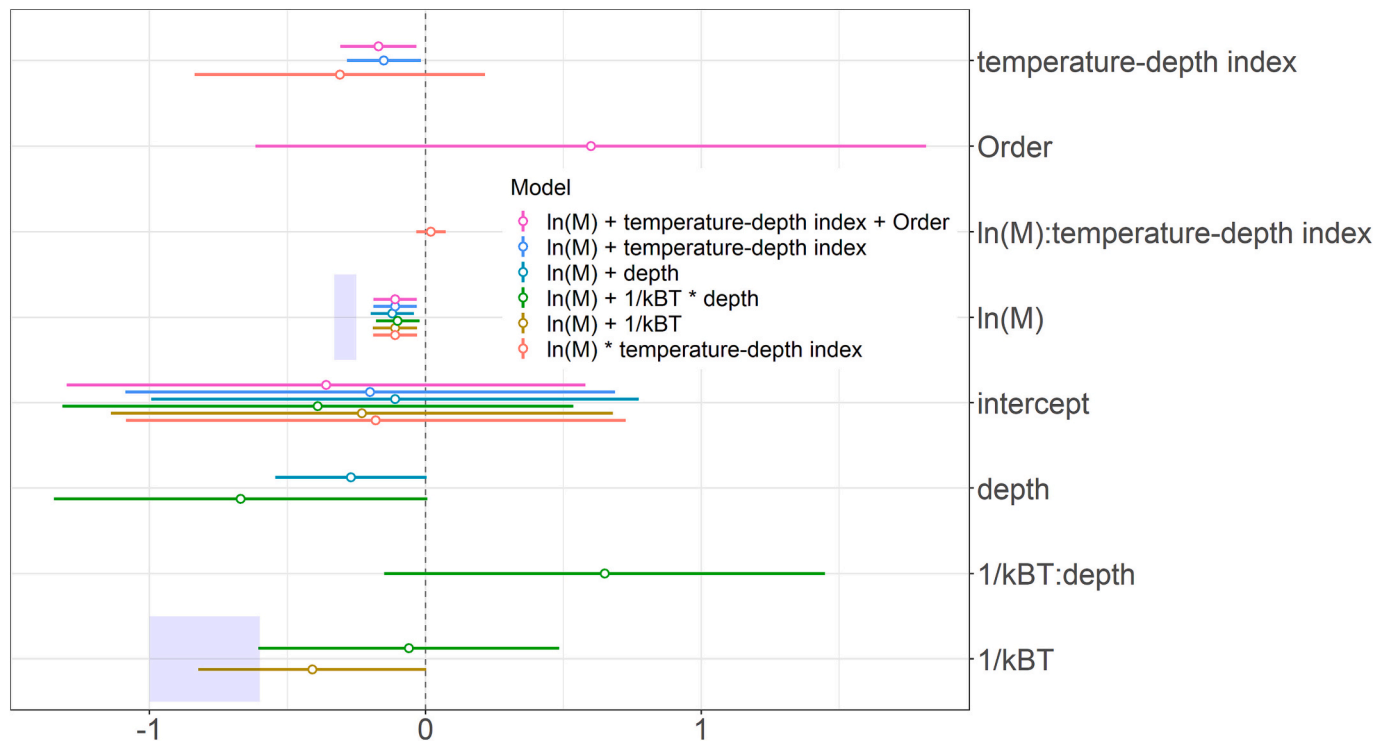| ln(r_{max}) ~	n	LL	AICc	adj_R_sq	ΔAICc	Weights
ln(M) + temperature-depth index	3	-65.4	137.2	0.14	0	0.177
ln(M) + temperature-depth index + Order	4	-65	138.4	0.14	1.2	0.097
ln(M) + $1/k_BT$	3	-66.1	138.5	0.12	1.3	0.092
ln(M) + depth	3	-66.1	138.6	0.12	1.4	0.088
ln(M) + $1/k_BT$ * depth	5	-64.1	138.9	0.14	1.7	0.076
ln(M) * temperature-depth index	4	-65.3	139.1	0.13	1.9	0.068
ln(M) + $1/k_BT$ + depth	4	-65.4	139.3	0.13	2.1	0.062
ln(M) + $1/k_BT$ + Order	4	-65.6	139.7	0.12	2.5	0.051
ln(M) * $1/k_BT$	4	-65.7	139.8	0.13	2.6	0.048
ln(M)	2	-68	140.2	0.09	3	0.039
ln(M) + depth + Order	4	-65.9	140.2	0.12	3	0.039
ln(M) * temperature-depth index + Order	5	-64.8	140.4	0.13	3.2	0.036
ln(M) * depth	4	-66.1	140.8	0.11	3.6	0.029
ln(M) * $1/k_BT$ + Order	5	-65.1	141	0.13	3.8	0.026
ln(M) + Order	3	-68	142.2	0.08	5	0.015
temperature-depth index	2	-69.1	142.3	0.07	5.1	0.014
ln(M) * depth + Order	5	-65.9	142.5	0.11	5.3	0.012
$1/k_BT$	2	-69.5	143.1	0.06	5.9	0.009
temperature-depth index + Order	3	-68.5	143.3	0.07	6.1	0.008
$1/k_BT$ + Order	3	-68.8	144	0.06	6.8	0.006
depth	2	-70.3	144.8	0.04	7.6	0.004
depth + Order	3	-70.1	146.4	0.04	9.2	0.002
1	1	-72.7	147.5	0	10.3	0.001
1 + Order	2	-72.6	149.4	-0.01	12.2	0

Fig. 3. Coefficient plots for the six models of ln(r_{max}) with AICc values < 2. Error bars show the 95 % confidence intervals, and effect sizes were considered significant when confidence intervals do not overlap zero. Shaded area shows the expected effect sizes for body mass (−0.33 to −0.25) and temperature (−1.0 to −0.6) based on metabolic scaling theory.

Table 3

Coefficient estimates (95 % confidence intervals estimated from standard errors shown in brackets) for all models of ln(r_{max}). The model with the lowest ΔAICc value is marked in bold and the models with ΔAIC < 2 are highlighted in grey. Pagel's λ indicates the strength of the phylogenetic signal.

ln(r_{max}) ~	intercept	ln(M)	depth	1/k_BT	ln(M):depth	ln(M):1/k_BT	Order	depth:1/k_BT	temperature-depth index	ln(M):temperature-depth index	Pagel's λ
1	-1.17 (-1.71 , -0.62)	-	-	-	-	-	-	-	-	-	0.88 (0.69 , 0.96)
1 + Order	-1.23 (-1.85 , -0.6)		-	-	-	-	0.25 (-1.05 , 1.55)	-	-	-	0.88 (0.68 , 0.96)
depth	-1.18 (-1.71 , -0.65)		-0.32 (-0.6 , -0.03)	-	-	-		-	-	-	0.88 (0.68 , 0.96)
depth + Order	-1.29 (-1.9 , -0.69)	-	-0.33 (-0.62 , -0.05)	-	-	-	0.47 (-0.8 , 1.73)	-	-	-	0.87 (0.65 , 0.96)
1/k_BT	-1.22 (-1.76 , -0.68)	-	-	-0.55 (-0.96 , -0.13)	-	-		-	-	-	0.89 (0.71 , 0.97)
1/k_BT + Order	-1.4 (-2.02 , -0.78)	-	-	-0.61 (-1.04 , -0.18)	-	-	0.74 (-0.57 , 2.05)	-	-	-	0.89 (0.68 , 0.97)
ln(M)	-0.01 (-0.91 , 0.89)	-0.12 (-0.2 , -0.05)	-	NA	-	-		-	-	-	0.88 (0.69 , 0.96)
ln(M) * depth	-0.1 (-1 , 0.79)	-0.12 (-0.2 , -0.04)	-0.30 (-1.75 , 1.15)	NA	0 (-0.15 , 0.16)	-	-	-	-	-	0.88 (0.63 , 0.96)
ln(M) * depth + Order	-0.21 (-1.16 , 0.73)	-0.12 (-0.19 , -0.04)	-0.29 (-1.75 , 1.17)	NA	0 (-0.16 , 0.16)	-	0.43 (-0.78 , 1.65)	-	-	-	0.87 (0.59 , 0.96)
ln(M) * 1/k_BT	-0.2 (-1.13 , 0.73)	-0.11 (-0.19 , -0.03)	-	-1.16 (-2.61 , 0.29)	NA	0.07 (-0.06 , 0.21)		-	-	-	0.92 (0.72 , 0.98)
ln(M) * 1/k_BT + Order	-0.39 (-1.39 , 0.61)	-0.11 (-0.19 , -0.03)	-	-1.26 (-2.73 , 0.21)	NA	0.08 (-0.06 , 0.22)	0.69 (-0.64 , 2.01)	-	-	-	0.91 (0.69 , 0.98)
ln(M) * temperature-depth index	-0.18 (-1.08 , 0.73)	-0.11 (-0.19 , -0.03)	-	-	-	-	-	-	-0.31 (-0.84 , 0.22)	0.02 (-0.04 , 0.07)	0.90 (0.67 , 0.97)
ln(M) * temperature-depth index + Order	-0.34 (-1.3 , 0.62)	-0.11 (-0.19 , -0.03)	-	-	-	-	0.61 (-0.65 , 1.86)	-	-0.32 (-0.85 , 0.21)	0.02 (-0.04 , 0.07)	0.89 (0.63 , 0.97)
ln(M) + depth	-0.11 (-0.99 , 0.78)	-0.12 (-0.19 , -0.04)	-0.27 (-0.55 , 0)	-	-	-	-	-	-	-	0.88 (0.67 , 0.96)
ln(M) + depth + Order	-0.21 (-1.15 , 0.72)	-0.12 (-0.19 , -0.04)	-0.29 (-0.57 , -0.01)	-	-	-	0.43 (-0.78 , 1.65)	-	-	-	0.87 (0.64 , 0.96)
ln(M) + 1/k_BT	-0.23 (-1.13 , 0.68)	-0.11 (-0.19 , -0.03)	-	-0.41 (-0.83 , 0)	-	-	-	-	-	-	0.89 (0.68 , 0.96)
ln(M) + 1/k_BT * depth	-0.39 (-1.31 , 0.54)	-0.10 (-0.18 , -0.02)	-0.67 (-1.35 , 0.01)	-0.06 (-0.6 , 0.49)	-	-	-	0.65 (-0.15 , 1.45)	-	-	0.89 (0.69 , 0.97)
ln(M) + 1/k_BT + depth	-0.22 (-1.13 , 0.68)	-0.11 (-0.19 , -0.03)	-0.18 (-0.49 , 0.13)	-0.28 (-0.75 , 0.19)	-	-		-	-	-	0.88 (0.67 , 0.96)
ln(M) + 1/k_BT + Order	-0.40 (-1.37 , 0.57)	-0.10 (-0.18 , -0.02)	-	-0.47 (-0.9 , -0.04)	-	-	0.63 (-0.63 , 1.88)	-	-	-	0.88 (0.65 , 0.96)
ln(M) + Order	-0.07 (-1.02 , 0.88)	-0.12 (-0.2 , -0.05)	-		-	-	0.25 (-0.99 , 1.49)	-	-	-	0.88 (0.68 , 0.96)
ln(M) + temperature-depth index	-0.20 (-1.09 , 0.69)	-0.11 (-0.19 , -0.03)	-	-	-	-	-	-	-0.15 (-0.29 , -0.02)	-	0.88 (0.67 , 0.96)
ln(M) + temperature-depth index + Order	-0.36 (-1.3 , 0.58)	-0.11 (-0.18 , -0.03)	-	-	-	-	0.60 (-0.62 , 1.81)	-	-0.17 (-0.31 , -0.03)	-	0.87 (0.63 , 0.96)
temperature-depth index	-1.21 (-1.74 , -0.68)							-	-0.19 (-0.32 , -0.05)	-	0.88 (0.69 , 0.96)
temperature-depth index + Order	-1.37 (-1.97 , -0.77)	-	-	-	-	-	0.67 (-0.59 , 1.94)	-	-0.21 (-0.35 , -0.07)		0.87 (0.65 , 0.96)

Generally, deep-water sharks have lower growth rates, later maturity, and greater longevity, with many live-bearing, deep-water sharks having a smaller body size and lower annual reproductive output (Rigby and Simpfendorfer, 2015). Consequently, r_{max} has been found to be lower in deep-water sharks compared to continental shelf and oceanic pelagic species (García et al., 2008). A similar pattern has been found using intrinsic rebound potentials, which is another measure of population growth rate (Simpfendorfer and Kyne, 2009; Smith et al., 1998). Expanding beyond these analyses that focussed on three categorical habitat types, Pardo and Dulvy (2022) investigated the effects of environmental temperature, depth, and mass scaling on r_{max} for sharks and rays. They found that deep-water species have a lower r_{max} due to the combined effects of cooler temperatures and an independent depth effect that could be due to multiple physiological and ecological factors, for example, lower secondary production at greater depths (Jahnke, 1996). To date, this literature has focussed on sharks in which the phylogenetic divergence between deep-water species (superorder Squalomorphii) and shallow-water species (superorder Galeomorphii) is relatively distant, for example, deep-water Dogfishes (Squaliformes) compared to shallow-water Horn Sharks (Heterodontiformes) and Mackerel Sharks (Lamniformes). Indeed, the hypothesised sequence of evolution is that ancestral sharks were deep-water species with small brains and low reproductive investment that subsequently gave rise to shallow-water lineages with lower fecundity and larger more complex brains (Compagno, 1990; Mull et al., 2020). In our analysis of rays and skates, we also found that r_{max} decreased with increasing depth and that this was mirrored by the relationship with temperature but that shallow-

water tropical rays still had a lower r_{max} relative to cold, deep-water temperate skates. Compared to sharks, the divergence between skates (Order Rajiformes) and other rays (Orders Myliobatiformes, Rhinopristiformes, and Torpediniformes) is more recent and clearly geographically defined, with the skates arising and radiating mainly in the Arctic polar and North Atlantic and North Pacific temperate latitudes and having a distinct pattern of egg-laying and much greater fecundity than the tropical rays (Frisk, 2010; McEachran and Miyake, 1990).

Instead of low temperature, we hypothesise the reason for slow life histories and low r_{max} estimates in deep-water sharks, such as Gulper Sharks (Centrophoridae), is their very low fecundity, typically less than five female offspring per year (Cotton et al., 2015; Graham and Daley, 2011; Paiva et al., 2011). Such low fecundity limits r_{max} and results in a low capacity for density-dependent compensation (Pardo et al., 2018). Similarly, many tropical rays have very low fecundity, notably the largest radiation of tropical rays: the Myliobatiformes. This Order has some species that produce only one to two very large offspring, no more frequently than once per year. For example, Devil rays (*Mobula* spp.) produce a single, large pup (rarely twins) born every 1–7 years (Marshall and Bennett, 2010; Rambahiniarison et al., 2018; White et al., 2006). Consequently, they have among the lowest r_{max} found for sharks and rays, as found in this and previous studies (Dulvy et al., 2014; Pardo et al., 2016a; Rambahiniarison et al., 2018). The fecundity of live-bearing shark and ray species more generally is lower when compared to egg-laying species of a similar body size, as they are limited by the size of the maternal body cavity given internal embryonic development (Musick and Ellis, 2005; Wourms and Lombardi, 1992). The study
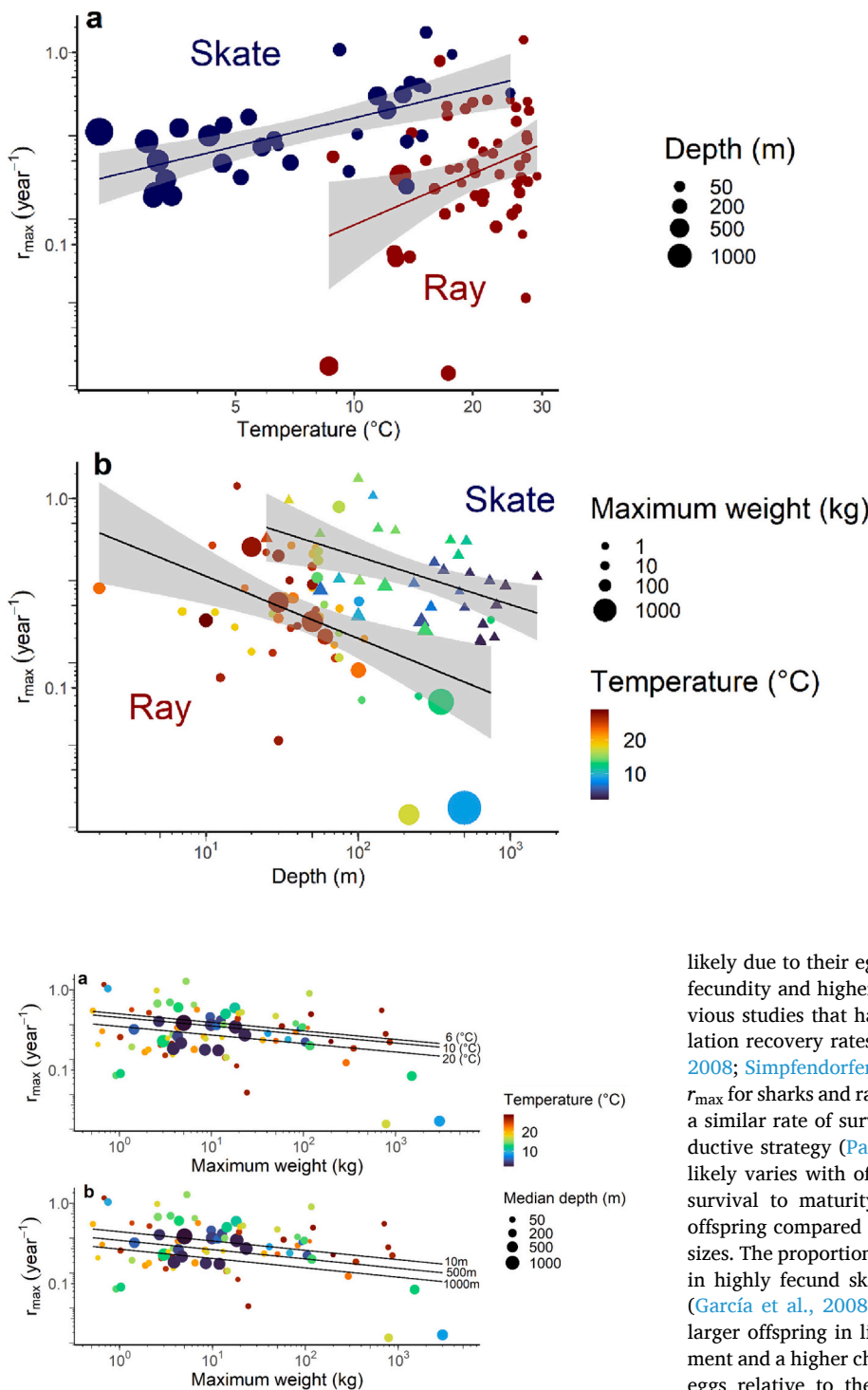
Fig. 4. Relationship between maximum intrinsic rate of population increase (r_{max}) and a) temperature (°C) and b) depth (m) in log10 space for 53 ray (Orders Myliobatiformes, Rhinopristiformes, and Torpediniformes) and 32 skate (Order Rajiformes) species. a) Median depth (m) is shown by the point size, with a linear model fitted to ray (red) and skate (blue) points. b) Median temperature (°C) and maximum weight (kg) are shown by the point colour and size, respectively, with a linear model fitted to ray (circular) and skate (triangular) data points. The grey band around the fitted models shows the confidence intervals. (For interpretation of the references to colour in this figure legend, the reader is referred to the web version of this article.)

Fig. 5. Relationship between maximum intrinsic rate of population increase (r_{max}) and body mass in log10 space for 85 ray and skate species. Fitted lines show predicted relationships based on the top-ranked models: a) $\ln(r_{max}) \sim \ln(M) + 1/k_B T$ and b) $\ln(r_{max}) \sim \ln(M) + $ depth. Predicted allometric changes of r_{max} across a) median temperatures (6, 10, 20 °C) and b) median depths (10, 500, 1000 m). Median temperature and depth are shown by the point colour and size, respectively. (For interpretation of the references to colour in this figure legend, the reader is referred to the web version of this article.)

results suggest that skates may be different to deep-water sharks that live longer, mature later, and have a lower annual reproductive output, and consequently are more intrinsically sensitive (Rigby and Simpfendorfer, 2015). This variation around expectations from metabolic theory is

likely due to their egg-laying reproductive strategy, resulting in higher fecundity and higher r_{max} (Pardo et al., 2018). This is in line with previous studies that have found higher extinction risk and slower population recovery rates in live-bearing, less fecund species (García et al., 2008; Simpfendorfer and Kyne, 2009). Previous methods of estimating r_{max} for sharks and rays have assumed all juveniles survive to maturity at a similar rate of survivorship in the adult stage, independent of reproductive strategy (Pardo et al., 2016b). However, juvenile survivorship likely varies with offspring size, in addition to lifespan, such that the survival to maturity may be greater in live-bearing rays with few offspring compared to fecund, egg-laying skates with smaller offspring sizes. The proportion of offspring that survive to maturity is likely lower in highly fecund skates, for example, due to predation on egg cases (García et al., 2008; Lucifora and García, 2004), compared to fewer, larger offspring in live-bearing rays that have higher maternal investment and a higher chance of survival (Frisk et al., 2001). The survival of eggs relative to the annual reproductive output (in the absence of density-dependence) is something that needs more investigation to further explore whether survival to maturity is truly comparable between these different reproductive strategies.

Skates in this study had a later median age at maturity, similar maximum age, but higher annual reproductive output compared to the rays. Whilst age at maturity has been found to be a major negative correlate of r_{max} (Hutchings et al., 2012), it is likely that the higher reproductive output is leading to higher r_{max} estimates, which may translate to lower intrinsic sensitivity. There will be a trade-off in energy investment in life history traits, such that offspring size is inversely related to fecundity, with less fecund species having larger offspring (Cortés, 2000). Recent work suggests that offspring size may be an important determinant of r_{max} (Denéchère et al., 2022). At the larger
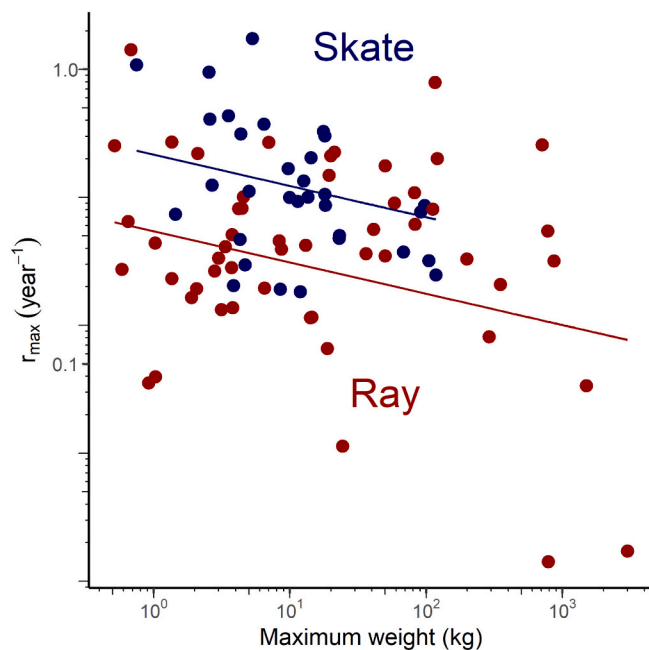
Fig. 6. Relationship between maximum intrinsic rate of population increase (r_{max}) and body mass in log10 space for 53 ray species (Orders Myliobatiformes, Rhinopristiformes, and Torpediniformes) and 32 skate species (Order Rajiformes). Fitted lines show predicted relationships based on the top-ranked model: $\ln(r_{max}) \sim \ln(M) +$ temperature-depth index $+$ Order. Predicted allometric changes of r_{max} across constant temperature-depth index (PC1 = 1) for ray (red) and skate (blue) data points. (For interpretation of the references to colour in this figure legend, the reader is referred to the web version of this article.)

taxonomic scale, there are broadly two breeding strategies in marine organisms: well-provisioned offspring that are proportional in size compared to the maternal body size, as seen generally in sharks and rays (Denéchère et al., 2022; Goodwin et al., 2002) and broadcast spawning in which offspring size (ovum diameter) is independent of maternal size and is typically 1–2 mm in diameter due to selection for pelagic dispersal in the plankton (as seen in teleosts; Duarte and Alcaraz, 1989). According to metabolic scaling theory, r_{max} scales with body mass with an exponent of $-1/4$ (Brown et al., 2004; Savage et al., 2004) but only when offspring size is proportional to adult size (Denéchère et al., 2022). Therefore, the paradox of lower r_{max} in warm-water rays could result from their larger offspring size (proportional to maternal body size) compared to the cooler-water skates, which lay pairs of eggs (mermaid's purses) that tend to be more consistently smaller in size despite a wide range in maternal sizes. Further, it would be interesting to explore differences in somatic growth rates between rays and skates as Denéchère et al. (2022) also found that there was variation around the $-1/4$ metabolic scaling expectation where somatic growth rates were proportional as opposed to independent of adult body mass (Denéchère et al., 2022).

Our finding that r_{max} is lower in the less fecund, tropical rays than the more fecund, cooler-dwelling skates, has profound consequences for fisheries sustainability and extinction risk. First, our findings imply that warm, shallow-water rays are more intrinsically sensitive to exploitation than the skates. Yet, historically skates have been at greater risk of extinction, with the loss of the largest bodied skates from both sides of the North Atlantic (Brander, 1981; Dulvy and Reynolds, 2002; Walker and Heessen, 1996). However, these relatively fecund species disappeared due to the intense trawl fisheries and the lack of management for skates. Now with reduction in fishing mortality and skate quotas, we are seeing stabilisation and recovery of larger skates (Bom et al., 2022; McGeady et al., 2022). At that time, there was little comparative

understanding of the state of tropical shark and ray fisheries. Over the past decade, it has become increasingly clear that tropical fisheries are particularly intense and relatively unregulated (Booth et al., 2019; Davidson et al., 2016; Sherman et al., 2023; Temple et al., 2019). The latest reassessment of all chondrichthyans has revealed greater threat in tropical coastal waters, with >75 % of tropical and subtropical coastal species threatened. Our result suggests that whilst this is mainly due to intense, largely unregulated fisheries, the differential intrinsic sensitivity of rays may go a long way to explain why batoid species are particularly at risk in the tropics (Dulvy et al., 2021; Temple et al., 2019). These results underscore the need for effective fisheries management, through catch and effort control (Blaber et al., 2009; Yulianto et al., 2018). Our estimates are at the global species level, yet many species are widely distributed and there is considerable evidence for geographic trait variation due to local adaptation (Cope, 2006). There might be temptation to wait until the data are gathered from the locale of interest before using these r_{max} estimates in risk analyses and other forms of management guidance. Instead, we remind that we estimated r_{max} based on 10,000 random deviates from a uniform distribution between minimum and maximum values of each life history parameter (or $\pm$ 10 % for α_{max}), hence, local population specific values are likely encompassed within the posterior distributions of the global species r_{max}. Hence, we recommend using the current values, as well as gathering more locale-specific life history data.

In addition to offspring size and survival, and the influence of offspring size on r_{max}, future research could explore (1) somatic growth rates and the different dimensions of reproductive output, such as offspring size, and their relationship with r_{max} to better understand the reasons behind the higher intrinsic sensitivity (lower r_{max}) found for tropical rays; (2) consider alternate temperature data to improve the estimation of r_{max}; and (3) access more data through imputation. First, this could include investigation of size-dependent mortality rates to account for offspring size and its effect on juvenile survival to maturity in estimations of r_{max} in order to investigate whether survival to maturity is truly comparable across reproductive strategies, such as between the live-bearing rays and egg-laying skates in this study. Further understanding of the relationship between offspring size and environmental temperature, given how the latter likely affects maternal investment, is also needed (Pettersen et al., 2019). Similarly, investigation of the relationship between r_{max} and somatic growth rate (von Bertalanffy k) or growth performance (Φ) relative to maternal size is required (Denéchère et al., 2022). A growth effect is likely correlated with temperature, with tropical species typically exhibiting faster growth rates and lower longevity. Variation in somatic growth has been found to be important alongside juvenile survival in population fluctuations of marine fishes (Stawitz and Essington, 2019). Second, we used a widely available temperature dataset to ensure that our approach was consistent with other recent papers and ongoing work (Pardo and Dulvy, 2022), however, in the future, it would be useful to explore the opportunity to average bottom temperatures for demersal species, for example, using Bio-Oracle or even using global climate models (Assis et al., 2018). The ability to use simple traits to understand r_{max} and subsequently, relative sensitivity to exploitation, recovery potential, and fishing limits, is crucial for data-poor species. This study provides the foundations for using body mass, environmental temperature, and depth to predict r_{max} for rays and skates and potentially for predicting future r_{max} estimates using global climate model projections. Future calculations will likely be able to utilise more data such as known occupied depth ranges and temperature profiles from tagged individuals. Third, with the rate of species and population decline and extinction, it is crucial that we use available trait information to predict extinction risk and guide conservation (Green et al., 2022). New Bayesian approaches can use the trait covariation on strength and variation of intercorrelations to impute missing trait values (Kindsvater et al., 2018). This has great potential to expand the range of species that can be considered in these analyses and has recently been used to estimate 59

unobserved traits for 23 populations of tunas and billfishes (Horswill et al., 2019).

5. Conclusions

The findings indicate that warm, shallow-water rays tend to be more intrinsically sensitive to exploitation than cold, deep-water skates; this is concerning given the greater extrinsic exposure to overfishing in shallow, tropical coastal waters. This may help explain why we are now finding that tropical and subtropical species are facing such a high threat of extinction and highlights the need for effective fisheries management. The use of simple life history traits, including maximum body size, environmental temperature, and depth range, in concert with phylogenetic imputation, may be a useful approach for estimating r_{max} for use in ecological risk assessments.

CRediT authorship contribution statement

Ellen Barrowclift: Conceptualisation, Methodology, Formal analysis, Investigation, Validation, Data curation, Writing- Original draft preparation, Writing- Review & Editing, Visualisation, Funding acquisition; Sarah M. Gravel: Formal analysis, Writing- Reviewing and Editing; Sebastián A. Pardo: Methodology, Formal analysis, Writing- Reviewing and Editing; Jennifer S. Bigman: Formal analysis, Writing- Reviewing and Editing; Per Berggren: Writing- Reviewing and Editing, Supervision, Funding acquisition; Nicholas K. Dulvy: Conceptualisation, Methodology, Formal analysis, Investigation, Validation, Data curation, Writing- Original draft preparation, Writing- Review & Editing, Visualisation, Funding acquisition, Supervision.

Declaration of competing interest

The authors declare that they have no known competing financial interests or personal relationships that could have appeared to influence the work reported in this paper.

Data availability statement

The collated database of life history data for the 85 batoid species analysed in this manuscript is available at Figshare (DOI: https://doi.org/10.6084/m9.figshare.20182109). Data and analysis code used to run the models in RStudio are available at GitHub (https://github.com/EBarrowclift/batoid-rmax-scaling).

Appendix A. Supplementary data

Supplementary data to this article can be found online at https://doi.org/10.1016/j.biocon.2023.110003.

References

Anderson, S.C., Farmer, R.G., Ferretti, F., Houde, A.L.S., Hutchings, J.A., 2011. Correlates of vertebrate extinction risk in Canada. Bioscience 61, 538–549. https://doi.org/10.1525/bio.2011.61.7.8.

Angilletta, M.J., Huey, R.B., Frazier, M.R., 2010. Thermodynamic effects on organismal performance: is hotter better? Physiol. Biochem. Zool. 83, 197–206. https://doi.org/10.1086/648567.

Arnold, T.W., 2010. Uninformative parameters and model selection using Akaike's information criterion. J. Wildl. Manag. 74, 1175–1178. https://doi.org/10.1111/j.1937-2817.2010.tb01236.x.

Assis, J., Tyberghein, L., Bosch, S., Verbruggen, H., Serrão, E.A., de Clerck, O., 2018. Bio-ORACLE v2.0: extending marine data layers for bioclimatic modelling. Glob. Ecol. Biogeogr. 27, 277–284. https://doi.org/10.1111/geb.12693.

Barbini, S.A., Sabadin, D.E., Román, J.M., Scarabotti, P.A., Lucifora, L.O., 2021. Age, growth, maturity and extinction risk of an exploited and endangered skate, *Atlantoraja castelnaui*, from off Uruguay and northern Argentina. J. Fish Biol. 99, 1328–1340. https://doi.org/10.1111/jfb.14839.

Barnett, L.A.K., Winton, M.v., Ainsley, S.M., Cailliet, G.M., Ebert, D.A., 2013. Comparative demography of skates: life-history correlates of productivity and implications for management. PLoS One 8, e65000. https://doi.org/10.1371/journal.pone.0065000.

Barrowclift, E., Temple, A.J., Stead, S., Jiddawi, N.S., Berggren, P., 2017. Social, economic and trade characteristics of the elasmobranch fishery on Unguja Island, Zanzibar, East Africa. Mar. Policy 83, 128–136. https://doi.org/10.1016/j.marpol.2017.06.002.

Béné, C., 2006. Small-scale fisheries: assessing their contribution to rural livelihoods in developing countries. In: FAO Fisheries Circular No. 1008.

Bernhardt, J.R., Sunday, J.M., O'Connor, M.I., 2018. Metabolic theory and the temperature-size rule explain the temperature dependence of population carrying capacity. Am. Nat. 192, 687–697. https://doi.org/10.1086/700114.

Blaber, S.J.M., Dichmont, C.M., White, W., Buckworth, R., Sadiyah, L., Iskandar, B., Nurhakim, S., Pillans, R., Andamari, R., Dharmadi, Fahmi, 2009. Elasmobranchs in southern Indonesian fisheries: the fisheries, the status of the stocks and management options. Rev. Fish Biol. Fish. 19, 367–391. https://doi.org/10.1007/s11160-009-9110-9.

Boettiger, C., Lang, D.T., Wainwright, P.C., 2012. rfishbase: exploring, manipulating and visualizing FishBase data from R. Journal of Fish Biology 81, 2030–2039. https://doi.org/10.1111/j.1095-8649.2012.03464.x.

Bom, R.A., Brader, A., Batsleer, J., Poos, J.J., van der Veer, H.W., van Leeuwen, A., 2022. A long-term view on recent changes in abundance of common skate complex in the North Sea. Mar. Biol. 169, 1–14. https://doi.org/10.1007/S00227-022-04132-w.

Booth, H., Squires, D., Milner-Gulland, E.J., 2019. The neglected complexities of shark fisheries, and priorities for holistic risk-based management. Ocean Coast. Manag. 182, 104994 https://doi.org/10.1016/j.ocecoaman.2019.104994.

Brander, K., 1981. Disappearance of common skate Raia batis from Irish Sea. Nature 290, 48–49. https://doi.org/10.1038/290048a0.

Brown, J.H., Gillooly, J.F., Allen, A.P., Savage, V.M., West, G.B., 2004. Toward a metabolic theory of ecology. Ecology 85, 1771–1789. https://doi.org/10.1890/03-9000.

Burnham, K.P., Anderson, D.R., 2002. Model Selection And Multimodel Inference: A Practical Information-Theoretic Approach, 2nd ed. Springer, New York. https://doi.org/10.1007/b97636.

Chichorro, F., Juslén, A., Cardoso, P., 2019. A review of the relation between species traits and extinction risk. Biol. Conserv. 237, 220–229. https://doi.org/10.1016/j.biocon.2019.07.001.

Clarke, A., 2017. Principles of Thermal Ecology; Temperature, Energy And Life. Oxford University Press. https://doi.org/10.1017/s0954102017000499. Cambridge University Press.

Clarke, A., Johnston, N.M., 1999. Scaling of metabolic rate with body mass and temperature in teleost fish. J. Anim. Ecol. 68, 893–905. https://doi.org/10.1046/j.1365-2656.1999.00337.x.

Compagno, L.J.v., 1990. Alternative life-history styles of cartilaginous fishes in time and space. Environ. Biol. Fish 28, 3–75.

Cope, J.M., 2006. Exploring intraspecific life history patterns in sharks. In: Fishery Bulletin, 104. National Oceanic and Atmospheric Administration, pp. 311–320.

Cortés, E., 2000. Life history patterns and correlations in sharks. Rev. Fish. Sci. 8, 299–344. https://doi.org/10.1080/10408340308951115.

Cortés, E., 2002. Incorporating uncertainty into demographic modeling: application to shark populations and their conservation. Conserv. Biol. 16, 1048–1062.

Cortés, E., 2016. Perspectives on the intrinsic rate of population growth. Methods Ecol. Evol. 7, 1136–1145. https://doi.org/10.1111/2041-210x.12592.

Cortés, E., Brooks, E.N., Shertzer, K.W., 2015. Risk assessment of cartilaginous fish populations. ICES J. Mar. Sci. 72, 1057–1068. https://doi.org/10.1093/icesjms/fsu157.

Cotton, C.F., Dean Grubbs, R., Dyb, J.E., Fossen, I., Musick, J.A., 2015. Reproduction and embryonic development in two species of squaliform sharks, Centrophorus granulosus and Etmopterus princeps: evidence of matrotrophy? Deep-Sea Res. II Top. Stud. Oceanogr. 115, 41–54. https://doi.org/10.1016/j.dsr2.2014.10.009.

D'Alberto, B.M., Carlson, J.K., Pardo, S.A., Simpfendorfer, C.A., 2019. Population productivity of shovelnose rays: inferring the potential for recovery. PLoS One 14. https://doi.org/10.1371/journal.pone.0225183.

Davidson, L.N.K., Krawchuk, M.A., Dulvy, N.K., 2016. Why have global shark and ray landings declined: improved management or overfishing? Fish Fish. 17, 438–458. https://doi.org/10.1111/faf.12119.

Denéchère, R., van Denderen, P.D., Andersen, K.H., 2022. Deriving population scaling rules from individual-level metabolism and life history traits. Am. Nat. 199, 564–575. https://doi.org/10.1086/718642.

Dillon, M.E., Wang, G., Huey, R.B., 2010. Global metabolic impacts of recent climate warming. Nature 467, 704–706. https://doi.org/10.1038/nature09407.

Dormann, C.F., Elith, J., Bacher, S., Buchmann, C., Carl, G., Carré, G., Marquéz, J.R.G., Gruber, B., Lafourcade, B., Leitão, P.J., Münkemüller, T., Mcclean, C., Osborne, P.E., Reineking, B., Schröder, B., Skidmore, A.K., Zurell, D., Lautenbach, S., 2013. Collinearity: a review of methods to deal with it and a simulation study evaluating their performance. Ecography 36, 27–46. https://doi.org/10.1111/j.1600-0587.2012.07348.x.

Duarte, C.M., Alcaraz, M., 1989. To produce many small or few large eggs: a size-independent reproductive tactic of fish. Oecologia 80, 401–404. https://doi.org/10.1007/bf00379043.

Dulvy, N., Forrest, R., 2010. Life histories, population dynamics, and extinction risks in chondrichthyans. In: Sharks And Their Relatives II: Biodiversity, Adaptive Physiology, And Conservation. CRC Press. https://doi.org/10.1201/9781420080483-c17.

Dulvy, N.K., Kindsvater, H.K., 2017. The future species of Anthropocene seas. In: Conservation for the Anthropocene Ocean: Interdisciplinary Science in Support of Nature and People, 39–64. https://doi.org/10.1016/B978-0-12-805375-1.00003-9.

Dulvy, N.K., Reynolds, J.D., 2002. Predicting extinction vulnerability in skates. Conserv. Biol. 16, 440–450. https://doi.org/10.1046/j.1523-1739.2002.00416.x.

Dulvy, N.K., Ellis, J.R., Goodwin, N.B., Grant, A., Reynolds, J.D., Jennings, S., 2004. Methods of assessing extinction risk in marine fishes. Fish Fish. 5, 255–276. https://doi.org/10.1111/j.1467-2679.2004.00158.x.

Dulvy, N.K., Pardo, S.A., Simpfendorfer, C.A., Carlson, J.K., 2014. Diagnosing the dangerous demography of manta rays using life history theory. PeerJ 2014, e400. https://doi.org/10.7717/peerj.400.

Dulvy, N.K., Pacoureau, N., Rigby, C.L., Pollom, R.A., Jabado, R.W., Ebert, D.A., Finucci, B., Pollock, C.M., Cheok, J., Derrick, D.H., Herman, K.B., Sherman, C.S., VanderWright, W.J., Lawson, J.M., Walls, R.H.L., Carlson, J.K., Charvet, P., Bineesh, K.K., Fernando, D., Ralph, G.M., Matsushiba, J.H., Hilton-Taylor, C., Fordham, S.v., Simpfendorfer, C.A., 2021. Overfishing drives over one-third of all sharks and rays toward a global extinction crisis. Curr. Biol. 31, 4773–4787.e8. https://doi.org/10.1016/j.cub.2021.08.062.

Fox, J., Weisberg, S., 2019. An R Companion to Applied Regression, Third edition. Sage, Thousand Oaks CA. https://socialsciences.mcmaster.ca/jfox/Books/Companion/.

Frisk, M., 2010. Life history strategies of batoids. In: Carrier, C., Musick, J.A., Heithaus, M.R. (Eds.), Sharks And Their Relatives II: Biodiversity, Adaptive Physiology, And Conservation. CRC Press, Boca Raton, pp. 283–316. https://doi.org/10.1201/9781420080483-c6.

Frisk, M.G., Miller, T.J., Fogarty, M.J., 2001. Estimation and analysis of biological parameters in elasmobranch fishes: a comparative life history study. Can. J. Fish. Aquat. Sci. 58, 969–981. https://doi.org/10.1139/cjfas-58-5-969.

FishBase. In: Froese, R., Pauly, D. (Eds.), 2022. World Wide Web electronic publication (08/2022). www.fishbase.org.

Froese, R., Thorson, J.T., Reyes, R.B., 2014. A Bayesian approach for estimating length-weight relationships in fishes. J. Appl. Ichthyol. 30, 78–85. https://doi.org/10.1111/jai.12299.

García, V.B., Lucifora, L.O., Myers, R.A., 2008. The importance of habitat and life history to extinction risk in sharks, skates, rays and chimaeras. Proc. R. Soc. B Biol. Sci. 275, 83–89. https://doi.org/10.1098/rspb.2007.1295.

Gedamke, T., Hoenig, J.M., Musick, J.A., DuPaul, W.D., Gruber, S.H., 2007. Using demographic models to determine intrinsic rate of increase and sustainable fishing for elasmobranchs: pitfalls, advances, and applications. N. Am. J. Fish Manag. 27, 605–618. https://doi.org/10.1577/m05-157.1.

Goodwin, N.B., Dulvy, N.K., Reynolds, J.D., 2002. Life-history correlates of the evolution of live bearing in fishes. Philos. Trans. R. Soc. Biol. Sci. 357, 259–267. https://doi.org/10.1098/rstb.2001.0958.

Graham, K.J., Daley, R.K., 2011. Distribution, reproduction and population structure of three gulper sharks (Centrophorus, Centrophoridae) in south-east Australian waters. Mar. Freshw. Res. 62, 583–595. https://doi.org/10.1071/mf10158.

Green, S.J., Brookson, C.B., Hardy, N.A., Crowder, L.B., 2022. Trait-based approaches to global change ecology: moving from description to prediction. Proc. R. Soc. B Biol. Sci. 289, 20220071. https://doi.org/10.1098/rspb.2022.0071.

Healy, K., Ezard, T.H.G., Jones, O.R., Salguero-Gómez, R., Buckley, Y.M., 2019. Animal life history is shaped by the pace of life and the distribution of age-specific mortality and reproduction. Nat. Ecol. Evol. 3, 1217–1224. https://doi.org/10.1038/s41559-019-0938-7.

Horswill, C., Kindsvater, H.K., Juan-Jordá, M.J., Dulvy, N.K., Mangel, M., Matthiopoulos, J., 2019. Global reconstruction of life-history strategies: a case study using tunas. J. Appl. Ecol. 56, 855–865. https://doi.org/10.1111/1365-2664.13327.

Hutchings, J.A., Myers, R.A., García, V.B., Lucifora, L.O., Kuparinen, A., 2012. Life-history correlates of extinction risk and recovery potential. Ecol. Appl. 22, 1061–1067. https://doi.org/10.1890/11-1313.1.

Jahnke, R.A., 1996. The global ocean flux of particulate organic carbon: areal distribution and magnitude. Glob. Biogeochem. Cycles 10, 71–88. https://doi.org/10.1029/95gb03525.

Jennings, S., Reynolds, J.D., Mills, S.C., 1998. Life history correlates of responses to fisheries exploitation. Proc. R. Soc. B Biol. Sci. 265, 333. https://doi.org/10.1098/rspb.1998.0300.

Jennings, S., Greenstreet, S.P.R., Reynolds, J.D., 1999. Structural change in an exploited fish community: a consequence of differential fishing effects on species with contrasting life histories. J. Anim. Ecol. 68, 617–627. https://doi.org/10.1046/j.1365-2656.1999.00312.x.

Juan-Jordá, M.J., Mosqueira, I., Freire, J., Dulvy, N.K., 2013. Life in 3-D: life history strategies in tunas, mackerels and bonitos. Rev. Fish Biol. Fish. 23, 135–155. https://doi.org/10.1007/s11160-012-9284-4.

Juan-Jordá, M.J., Mosqueira, I., Freire, J., Dulvy, N.K., 2015. Population declines of tuna and relatives depend on their speed of life. Proc. R. Soc. B Biol. Sci. 282 https://doi.org/10.1098/RSPB.2015.0322.

Kindsvater, H.K., Dulvy, N.K., Horswill, C., Juan-Jordá, M.J., Mangel, M., Matthiopoulos, J., 2018. Overcoming the data crisis in biodiversity conservation. Trends Ecol. Evol. 33, 676-688. https://doi.org/10.1016/j.tree.2018.06.004.

Lucifora, L.O., García, V.B., 2004. Gastropod predation on egg cases of skates (Chondrichthyes, Rajidae) in the southwestern Atlantic: quantification and life history implications. Mar. Biol. 145, 917–922. https://doi.org/10.1007/s00227-004-1377-8.

Lucifora, L.O., Scarabotti, P.A., Barbini, S.A., 2022. Predicting and contextualizing sensitivity to overfishing in Neotropical freshwater stingrays (Chondrichthyes: Potamotrygonidae). Rev. Fish Biol. Fish. 32, 669–686. https://doi.org/10.1007/S11160-021-09696-2.

Luhring, T.M., Delong, J.P., 2017. Scaling from metabolism to population growth rate to understand how acclimation temperature alters thermal performance. Integr. Comp. Biol. 57, 103–111. https://doi.org/10.1093/icb/icx041.

Marshall, A.D., Bennett, M.B., 2010. Reproductive ecology of the reef manta ray Manta alfredi in southern Mozambique. J. Fish Biol. 77, 169–190. https://doi.org/10.1111/j.1095-8649.2010.02669.x.

Martell, S., Froese, R., 2013. A simple method for estimating MSY from catch and resilience. Fish Fish. 14, 504–514. https://doi.org/10.1111/j.1467-2979.2012.00485.x.

McEachran, J., Miyake, T., 1990. Zoogeography and Bathymetry of skates (Chondrichthyes, Rajoidei), Elasmobranchs as living resources: advances in the biology, ecology, systematics, and the status of the fisheries. In: NOAA Technical Report National Marine Fisheries Service 90.

McGeady, R., Loca, S.L., McGonigle, C., 2022. Spatio-temporal dynamics of the common skate species complex: evidence of increasing abundance. Divers. Distrib. 28, 2403–2415. https://doi.org/10.1111/ddi.13635.

Mull, C., Pacoureau, N., Pardo, S., Saldaña Ruiz, L., Rodriguez, E., Finucci, B., Haack, M., Harry, A., Judah, A., VanderWright, W., Yin, J., Kindsvater, H., Dulvy, N., 2022. Sharkipedia: a curated open-access database of shark and ray life history traits and abundance time-series. Sci. Data 9. https://doi.org/10.1038/s41597-022-01655-1.

Mull, C.G., Yopak, K.E., Dulvy, N.K., 2020. Maternal investment, ecological lifestyle, and brain evolution in sharks and rays. Am. Nat. 195, 1056–1069. https://doi.org/10.5061/dryad.kprr4xh1b.

Musick, J.A., Ellis, J.K., 2005. Reproductive evolution of chondrichthyans. In: Hamlett, W.C. (Ed.), Reproductive Biology And Phylogeny of Chondrichthyes. CRC Press, Boca Raton, pp. 45–78.

Myers, R.A., Mertz, G., Fowlow, P.S., 1997. Maximum population growth rates and recovery times for Atlantic cod, Gadus morhua. Fish. Bull. 95, 762–772.

Myers, R.A., Bowen, K.G., Barrowman, N.J., 1999. Maximum reproductive rate of fish at low population sizes. Can. J. Fish. Aquat. Sci. 56, 2404–2419. https://doi.org/10.1139/f99-201.

Orme, D., Freckleton, R., Thomas, G., Petzoldt, T., Fritz, S., Isaac, N., Pearse, W., 2018. caper: Comparative Analyses of Phylogenetics And Evolution in R.

Paiva, R.B., Neves, A., Sequeira, V., Gordo, L., 2011. Reproductive parameters of the commercially exploited deep-water shark, Deania calcea (Centrophoridae). Cybium 2, 131–140.

Pardo, S.A., Dulvy, N.K., 2022. Body mass, temperature, and depth shape the maximum intrinsic rate of population increase in sharks and rays. Ecol. Evol. https://doi.org/10.1002/ece3.9441 doi:10.1101/2021.03.02.433372.

Pardo, S.A., Kindsvater, H.K., Cuevas-Zimbrón, E., Sosa-Nishizaki, O., Carlos Pérez-Jiménez, J., Dulvy, N.K., 2016a. Growth, productivity, and relative extinction risk of a data-sparse devil ray. Sci. Rep. 6, 33745. https://doi.org/10.1038/srep33745.

Pardo, S.A., Kindsvater, H.K., Reynolds, J.D., Dulvy, N.K., 2016b. Maximum intrinsic rate of population increase in sharks, rays, and chimaeras: the importance of survival to maturity. Can. J. Fish. Aquat. Sci. 73, 1159–1163. https://doi.org/10.1139/cjfas-2016-0069.

Pardo, S.A., Cooper, A.B., Reynolds, J.D., Dulvy, N.K., 2018. Quantifying the known unknowns: estimating maximum intrinsic rate of population increase in the face of uncertainty. ICES J. Mar. Sci. 75, 953–963. https://doi.org/10.1093/icesjms/fsx220.

Patrick, W.S., Spencer, P., Link, J., Cope, J., Field, J., Kobayashi, D., Lawson, P., Gedamke, T., Cortés, E., Ormseth, O., Bigelow, K., Overholtz, W., 2010. Using productivity and susceptibility indices to assess the vulnerability of United States fish stocks to overfishing. Fish. Bull. 108, 305–322.

Pauly, D., 2006. Major trends in small-scale marine fisheries, with emphasis on developing countries, and some implications for the social sciences. Mar.Stud. 4, 7–22.

Pettersen, A.K., White, C.R., Bryson-Richardson, R.J., Marshall, D.J., 2019. Linking life-history theory and metabolic theory explains the offspring size-temperature relationship. Ecol. Lett. 22, 518–526. https://doi.org/10.1111/ele.13213.

Pörtner, H., 2001. Climate change and temperature-dependent biogeography: oxygen limitation of thermal tolerance in animals. Naturwissenschaften 88, 137–146. https://doi.org/10.1007/s001140100216.

Powter, D.M., Gladstone, W., 2008. Embryonic mortality and predation on egg capsules of the Port Jackson shark Heterodontus portusjacksoni (Meyer). J. Fish Biol. 72, 573–584. https://doi.org/10.1111/j.1095-8649.2007.01721.x.

Quetglas, A., Rueda, L., Alvarez-Berastegui, D., Guijarro, B., Massutí, E., 2016. Contrasting responses to harvesting and environmental drivers of fast and slow life history species. PLoS One 11, e0148770. https://doi.org/10.1371/journal.pone.0148770.

R Core Team, 2021. R: A Language And Environment for Statistical Computing. R Foundation for Statistical Computing, Vienna, Austria.

Rambahiniarison, J.M., Lamoste, M.J., Rohner, C.A., Murray, R., Snow, S., Labaja, J., Araujo, G., Ponzo, A., 2018. Life history, growth, and reproductive biology of four mobulid species in the Bohol Sea,Philippines. Front. Mar. Sci. 5, 269. https://doi.org/10.3389/fmars.2018.00269.

Revell, L.J., 2010. Phylogenetic signal and linear regression on species data. Methods Ecol. Evol. 1, 319–329. https://doi.org/10.1111/j.2041-210x.2010.00044.x.

Reynolds, J.D., 2003. Life histories and extinction risk. In: Macroecology. Blackwell Publishing, Oxford.

Reynolds, J.D., Dulvy, N.K., Goodwin, N.B., Hutchings, J.A., 2005. Biology of extinction risk in marine fishes. Proc. R. Soc. B Biol. Sci. 272, 2337–2344. https://doi.org/10.1098/rspb.2005.3281.

Rigby, C., Simpfendorfer, C.A., 2015. Patterns in life history traits of deep-water chondrichthyans. Deep-Sea Res. II Top. Stud. Oceanogr. 115, 30–40. https://doi.org/10.1016/j.dsr2.2013.09.004.

RStudio Team, 2021. RStudio: Integrated Development Environment for R. RStudio, PBC, Boston, MA.

Savage, V.M., Gillooly, J.F., Brown, J.H., West, G.B., Charnov, E.L., 2004. Effects of body size and temperature on population growth. Am. Nat. 163, 429–441. https://doi.org/10.1086/381872.

Sherman, C., Digel, E., Zubick, P., Eged, J., Haque, A., Matsushiba, J., Simpfendorfer, C., Sant, G., Dulvy, N., 2023. High overexploitation risk and management shortfall in highly traded requiem sharks. Conserv. Lett. e12940 https://doi.org/10.1111/conl.12940.

Simpfendorfer, C.A., Dulvy, N.K., 2017. Bright spots of sustainable shark fishing. Curr. Biol. 27, R97–R98. https://doi.org/10.1016/j.cub.2016.12.017.

Simpfendorfer, C.A., Kyne, P.M., 2009. Limited potential to recover from overfishing raises concerns for deep-sea sharks, rays and chimaeras. Environ. Conserv. 36, 97–103. https://doi.org/10.1017/s0376892909990191.

Smith, S.E., Au, D.W., Show, C., 1998. Intrinsic rebound potentials of 26 species of Pacific sharks. Mar. Freshw. Res. 49, 663–678. https://doi.org/10.1071/mf97135.

Stawitz, C.C., Essington, T.E., 2019. Somatic growth contributes to population variation in marine fishes. J. Anim. Ecol. 88, 315–329. https://doi.org/10.1111/1365-2656.12921.

Stein, R.W., Mull, C.G., Kuhn, T.S., Aschliman, N.C., Davidson, L.N.K., Joy, J.B., Smith, G.J., Dulvy, N.K., Mooers, A.O., 2018. Global priorities for conserving the evolutionary history of sharks, rays and chimaeras. Nat. Ecol. Evol. 2, 288–298. https://doi.org/10.1038/s41559-017-0448-4.

Temple, A.J., Wambiji, N., Poonian, C.N.S., Jiddawi, N., Stead, S.M., Kiszka, J.J., Berggren, P., 2019. Marine megafauna catch in southwestern Indian Ocean small-scale fisheries from landings data. Biol. Conserv. 230, 113–121. https://doi.org/10.1016/j.biocon.2018.12.024.

Temple, A.J., Stead, S.M., Jiddawi, N., Wambiji, N., Dulvy, N.K., Barrowclift, E., Berggren, P., 2020. Life-history, exploitation and extinction risk of the data-poor Baraka's whipray (Maculabatis ambigua) in small-scale tropical fisheries. J. Fish Biol. 1–12 https://doi.org/10.1111/jfb.14425.

Walker, P.A., Heessen, H.J.L., 1996. Long-term changes in ray populations in the North Sea. ICES J. Mar. Sci. 53, 1085–1093. https://doi.org/10.1006/jmsc.1996.0135.

Ward-Paige, C.A., 2017. A global overview of shark sanctuary regulations and their impact on shark fisheries. Mar. Policy 82, 87–97. https://doi.org/10.1016/j.marpol.2017.05.004.

Webb, T.J., Dulvy, N.K., Jennings, S., Polunin, N.V.C., 2011. The birds and the seas: body size reconciles differences in the abundance–occupancy relationship across marine and terrestrial vertebrates. Oikos 120, 537–549. https://doi.org/10.1111/j.1600-0706.2011.18870.x.

White, C.R., Alton, L.A., Bywater, C.L., Lombardi, E.J., Marshall, D.J., 2022. Metabolic scaling is the product of life-history optimization. Science 1979 (377), 834–839. https://doi.org/10.1126/science.abm7649.

White, W.T., Giles, J., Dharmadi, Potter, I.C., 2006. Data on the bycatch fishery and reproductive biology of mobulid rays (Myliobatiformes) in Indonesia. Fish. Res. 82, 65–73. https://doi.org/10.1016/j.fishres.2006.08.008.

Wong, S., Bigman, J.S., Dulvy, N.K., 2021. The metabolic pace of life histories across fishes. Proc. R. Soc. B Biol. Sci. 288 https://doi.org/10.1098/rspb.2021.0910.

Wourms, J.P., 1977. Reproduction and development in chondrichthyan fishes. Integr. Comp. Biol. 17, 379–410. https://doi.org/10.1093/icb/17.2.379.

Wourms, J.P., Lombardi, J., 1992. Reflections on the evolution of piscine viviparity. Am. Zool. 32, 276–293. https://doi.org/10.1093/icb/32.2.276.

Yan, H.F., Kyne, P.M., Jabado, R.W., Leeney, R.H., Davidson, L.N.K., Derrick, D.H., Finucci, B., Freckleton, R.P., Fordham, S.V., Dulvy, N.K., 2021. Overfishing and habitat loss drive range contraction of iconic marine fishes to near extinction. Sci. Adv. 7, 6026. https://doi.org/10.1126/sciadv.abb60.

Yulianto, I., Booth, H., Ningtias, P., Kartawijaya, T., Santos, J., Sarmintohadi, Kleinertz, S., Campbell, S.J., Palm, H.W., Hammer, C., 2018. Practical measures for sustainable shark fisheries: lessons learned from an Indonesian targeted shark fishery. PLoS One 13. https://doi.org/10.1371/journal.pone.0206437.